ORIGINAL ARTICLE

In Vivo Brain Concentrations of *N*-Acetyl Compounds, Creatine, and Choline in Alzheimer Disease

Adolf Pfefferbaum, MD; Elfar Adalsteinsson, PhD; Daniel Spielman, PhD; Edith V. Sullivan, PhD; Kelvin O. Lim, MD

Background: Alzheimer disease (AD) and normal aging result in cortical gray matter volume deficits. The extent to which the remaining cortex is functionally compromised can be estimated in vivo with magnetic resonance spectroscopic imaging.

Objective: To assess the effects of age and dementia on gray matter and white matter concentrations of 3 metabolites visible in the proton spectrum: *N*-acetyl compounds, present only in living neurons; creatine plus phosphocreatine, reflecting high-energy phosphate metabolism; and choline, increasing with membrane synthesis and degradation.

Method: Fifteen healthy young individuals, 19 healthy elderly individuals, and 16 patients with AD underwent 3-dimensional magnetic resonance spectroscopic imaging and memory and language testing.

Results: Gray matter *N*-acetyl compound concentrations (signal intensity corrected for the amount of brain tissue contributing to the magnetic resonance spectroscopic imaging signal) was significantly reduced only in patients with AD, even though both the AD and elderly control groups had substantial gray matter volume deficits relative to the young control group. Both the healthy elderly and AD groups had abnormally high gray matter creatine plus phosphocreatine concentrations. Gray matter choline concentrations were higher in the elderly than the younger controls, and even higher in the AD group than in the elderly control group. Functional significance of these findings was supported by correlations between poorer performance on recognition memory tests and lower gray matter *N*-acetyl compounds in elderly controls and higher gray matter creatine plus phosphocreatine and choline concentrations in patients with AD.

Conclusion: Cortical gray matter volume deficits in patients with AD are accompanied by disease-related increases in gray matter choline concentrations suggestive of cellular degeneration and reduced *N*-acetyl compound concentrations, with possible effects on behavioral function.

Arch Gen Psychiatry. 1999;56:185-192

From the Neuropsychiatry Program, SRI International, Menlo Park (Dr Pfefferbaum); Departments of Psychiatry and Behavioral Sciences (Drs Pfefferbaum and Sullivan) and Radiology (Drs Adalsteinsson and Spielman), Stanford University School of Medicine, Stanford, Calif; and the Nathan Kline Institute, Orangeburg, NY (Dr Lim).

ALZHEIMER DISEASE (AD) results in substantial loss of brain tissue.[1-15] This decline is attributable to deterioration of cell processes, shrinkage of neurons, and perhaps neuronal death.[10,16-20] Healthy elderly individuals show an age-related gray matter volume decline in the neocortex[21-24] (see Guttman et al[25]) but their volume loss may not be accompanied by neuronal death.[26-29] At issue is the functionality of the tissue remaining in the brains of healthy elderly patients and patients with AD.

In vivo proton magnetic resonance spectroscopic imaging (^{1}H MRSI) allows examination of brain tissue integrity. The *N*-acetyl (NAc) peak is composed of several NAc compounds, including NAc aspartate, that are present only in living, mature neurons and not glia.[30] Many studies have reported lower NAc signals in patients with AD compared with healthy elderly individuals [31-33]; some,[34-37] but not others,[38-43] have reported age-related decline in brain NAc in healthy people. Most studies have employed single-voxel spectroscopy[31] and have expressed NAc as a ratio[44-47] of 1 or 2 other metabolites: creatine plus phosphocreatine (Cr), which reflects high-energy phosphate metabolism, and choline (Cho), which increases in signal intensity with membrane synthesis and degradation.[48,49] Many proton spectroscopy studies assume that neither age nor AD seriously affects Cr or Cho levels and thus express data as ratios.

We developed an MRSI method to estimate absolute proton metabolite signal intensities in gray matter and white matter separately.[38] Concentration, expressed

PARTICIPANTS AND METHODS

The 3 study groups included 15 young controls (all men; mean [± SD] age, 25.3 ± 2.9 years), 19 healthy elderly controls (9 men, 10 women; mean age, 73.3 ± 4.1 years), and 16 patients with AD (6 men, 10 women; mean age, 73.4 ± 6.0 years). All analyses were performed blind to subject identity.

The patients with AD were recruited from the Geriatric Psychiatry Rehabilitation Unit and the National Institute of Mental Health Aging Clinical Research Center at the Veterans Affairs Palo Alto Health Care System, Palo Alto, Calif (**Table 1**). These centers have a 90.2% autopsy-confirmed AD success rate of patients who in life had a diagnosis of probable AD. Patients met National Institute of Neurological and Communicative Diseases and Stroke–Alzheimer's Disease and Related Disorders Association criteria for probable Alzheimer disease.[61,62] Controls were recruited from the local community. Subjects were excluded if they had any significant history of psychiatric or neurological disorder unrelated to their diagnosis (stroke, closed head injury), current alcohol or other drug abuse or dependence, or a life-threatening medical condition. Screening included a psychiatric interview and medical examination; informed consent was obtained from all participants (Table 1).

The elderly control and AD groups were matched in age and sex, were comparable in years of education (elderly control mean [± SD], 16.3 ± 2.2 years; AD mean, 15.4 ± 2.0 years), and achieved similar scores on the National Adult Reading Test, an estimate of premorbid intelligence (elderly control mean [± SD], 115.6 ± 5.8; AD mean, 110.6 ± 9.5). Patients with AD (mean [± SD] score, 19.8 ± 4.6) had significantly lower scores than the elderly controls (mean score, 28.5 ± 1.2) on the Mini-Mental State Examination.[63]

NEUROPSYCHOLOGICAL TESTS

Cognitive data were collected within 3 months (0-84 days) of magnetic resonance imaging. Brain-behavior relationships were based on tests assessing verbal and nonverbal recognition and word finding. The Warrington Recognition Test[64] assessed memory for words and faces, and the modified Boston Naming Test[65] assessed confrontation naming.

IMAGE ACQUISITION

In vivo proton MRSI and structural magnetic resonance imaging scans were acquired using a quadrature head coil on a 1.5-T magnetic resonance imaging scanner (5.6 System software; GE Signa, Milwaukee, Wis) with echo-speed gradient hardware (GE Medical Systems; Milwaukee, Wis) (2.2-G/cm maximum gradient amplitude, and 185-µs minimum rise time). Data were obtained with oblique anatomic prescriptions parallel to the anteroposterior commissure (AC-PC) line identified from midsagittal structural images. The image acquisition protocol and analysis are given in other studies.[38]

Spectroscopic Image Acquisition

A modified version of a 3-dimensional MRSI sequence using a time-varying readout gradient in the slice selection direction was used to image multiple contiguous slices.[66] Excitation was accomplished with a pair of spin-echo, spectral-spatial pulses preceded by an adiabatic inversion as described in other studies.[38] Collection parameters were repetition time (TR), 2 seconds; inversion time (TI), 170 milliseconds; echo time (TE), 144 milliseconds. The nominal voxel size was 1.1 cm^3 and the total MRSI time was 17 minutes. Data reconstruction and metabolite estimation were performed as described elsewhere.[66] Corrections for receiver gain and coil loading were made when images were reconstructed to allow comparability of metabolite signal levels between subjects.[41] The final metabolite images were 16 images of 32×32 pixels each.

Shimming and Fieldmap Acquisition

An automated shimming procedure[67,68] with 3 linear terms and 6 nonlinear terms was used to minimize main field variations. A final 3-dimensional fieldmap was collected at a resolution of 64×64×32 voxels (TR, 40 milliseconds; and TE, 10 milliseconds; flip angle, 20°; effective slice thickness, 6.4 mm; and field of view, 24 cm) to measure residual field inhomogeneities.

as institutional signal intensity units per tissue volume, revealed more NAc in gray matter than white matter, consistent with many, [34,50-56] but not all,[57-60] studies. Despite significant gray matter volume deficits in elderly healthy individuals, the young and elderly groups had equivalent concentrations of NAc in gray matter and white matter. By contrast, Cr and Cho concentrations demonstrated significant age effects. Cho concentrations were greater in gray matter in older controls; Cr concentrations were greater in gray matter and white matter in older subjects. These observations draw into question the use of Cr and Cho as appropriate referents for determining NAc concentration.

We applied our MRSI method to patients with AD and compared their results with those from our study of normal aging.[38] We expected the patients with AD, unlike the healthy elderly controls, to have abnormally low NAc concentrations in gray matter and white matter. We also anticipated that Cho levels would be even higher in patients with AD than they were in healthy elderly controls.

RESULTS

BRAIN TISSUE VOLUMES

The patients with AD had smaller gray matter volumes than the elderly controls, who had smaller volumes than the young controls ($F_{2,49} = 115.904$, $P = .001$). Cerebrospinal fluid volumes showed a complementary stepwise group effect ($F_{2,49} = 70.966$, $P = .001$). The overall group difference was significant for white matter ($F_{2,49} = 3.476$, $P = .04$), but only the AD group exhibited a volume deficit relative to the young and the elderly control groups (**Figure 2**). The pattern of group differences was virtually identical when examining only those

Structural Image Acquisition

A midsagittal, gradient-recalled echo image was used to compute slice positions with 0.5-mm accuracy for all 3 scans in this protocol (anatomical, fieldmap, and MRSI). Anatomic images were acquired with an axial fast-spin echo protocol (TR, 3000 milliseconds; and TE, 20/80 milliseconds; echo train length, 8; 3-mm skip, 0.2 mm; 256 × 256 pixels matrix; field of view, 24 cm; number of excitations, 1; and time, 3 minutes 18 seconds). Sixteen slices were collected, the most inferior slice beginning at the anteroposterior commissure line, corresponding to the 8 middle spectroscopic slices and providing 2 anatomical slices for each MRSI slice. Twelve of these high-resolution images, corresponding to 6 slices of metabolite data, were used in the structure/metabolite analysis.

An average imaging session with the above-described protocol took about 1 hour.

IMAGE ANALYSIS

Spectroscopic Images

Six MRSI slices were used, beginning with the slice 12.8 mm above the anteroposterior commissure line and extending superiorly (**Figure 1**). These slices were chosen because they had the least amount of signal loss and artifacts due to field inhomogeneity. Within these 6 slices, only pixels with good homogeneity (B_0 shifts within the range of ± 5 Hz) were included for analysis. These slices were also manually edited to remove regions, usually outside of the brain, of obvious lipid and/or water artifacts. To further guard against the possibility that incompletely suppressed water signal contaminated the MRSI data, especially for Cho and Cr concentrations in the medial frontal region, an exclusion region roughly corresponding to the cingulate gyrus was constructed for each slice by proportionate geometric positioning. The metabolite signals were calculated as magnitude values, so the noise in the metabolite maps had a nongaussian (Rician) noise distribution in the low signal-to-noise ratio range. To account for the effects of this nongaussian noise distribution, a bias correction was applied to the metabolite signal intensity values.[69]

Structural Images

Nonbrain (ie, dura, skull, and scalp) tissue was removed. The images were converted into segmentation maps, with each pixel designated as gray matter, white matter, or cerebrospinal fluid, and volumes were derived for each compartment. The data from each of the 2 segmented, high-resolution, structural slices corresponding to a metabolite slice were combined to provide 128 (8×8×2) segmented voxels underlying each metabolite voxel. Brain tissue composition of each subject was computed, with and without the voxels excluded in the metabolite analysis (Figure 1).

Structural and Metabolite Image Analysis

The segmented structural data were filtered to yield the same spatial frequency characteristics as the MRSI data. The optimum gray matter and white matter NAc, Cr, and Cho levels were found using a robust, least absolute deviation–regression algorithm.[38] The metabolite spectrum in each voxel was assumed to be a combination of signals from tissue compartments of gray matter and white matter. The gray matter and white matter tissue composition of each spectroscopic voxel was calculated from the segmented structural data. Given this information, the signal intensity of both gray matter and white matter was estimated for each subject and each metabolite.

STATISTICAL ANALYSIS

Group differences were tested with repeated-measures analysis of variance and Student *t* tests. We performed exploratory correlations between metabolite measures and cognitive test scores with Pearson product-moment correlations. We report correlations that reached $P<.05$ or less (1 tailed), with predictions that better performance would be associated with higher concentrations of NAc and lower concentrations of Cr and Cho; family-wise Bonferonni adjustment for 3 comparisons (3 tests for each metabolite) required $P<.03$. Correlations were done for the AD and elderly control groups independently to avoid the possibility that the results would merely reflect group differences.

structural voxels that corresponded to the spectroscopic voxels meeting the inclusion criteria (**Table 2**).

METABOLITE CONCENTRATION AND TISSUE TYPE

Despite the significant tissue volume deficit in patients with AD, the number of spectroscopic voxels meeting criteria for analysis did not differ significantly among the 3 groups ($F_{2,49}=2.399$, $P=.10$). The concentration estimation model provided separate metabolite concentration estimates for gray matter and white matter (**Figure 3**).

A repeated-measures analysis of variance (3 groups by 2 tissue types) for NAc concentration yielded significant effects of group ($F_{2,47}=6.913$, $P=.002$) and tissue type ($F_{2,47}=234.108$, $P=.001$) but no interaction ($F_{2,47}=1.708$, $P=.19$). The overall group difference was significant in gray matter ($F_{2,49}=5.283$, $P=.008$); the AD group had significantly lower gray matter NAc levels than the young ($P=.03$) and elderly ($P=.009$) control groups, which did not differ from each other. The ratio of gray to white matter NAc concentration was similar for the 3 groups (young control ratio = 1.31; elderly control ratio = 1.38; and patients with AD ratio = 1.30) ($F_{2,49}=1.024$, $P=.37$).

For Cr concentration, a repeated-measures analysis of variance (3 groups by 2 tissue types) yielded significant group ($F_{2,47}=21.25$, $P=.001$) and tissue-type effects ($F_{1,47}=884.214$, $P=.001$) and interaction ($F_{2,47}=3.934$, $P=.03$). For both tissue types, the elderly controls and patients with AD had higher Cr concentrations than the young controls (elderly vs young controls for gray matter: $t_{32}=4.678$, $P=.001$, and for white matter: $t_{32}=3.935$, $P=.001$; patients with AD vs young controls for gray matter: $t_{29}=4.619$, $P=.001$, and for white matter: $t_{29}=2.572$, $P=.02$). By contrast, the elderly con-

trol and AD groups did not differ significantly from each other in either gray matter ($t_{33} = 1.065$, $P = .29$) or white matter ($t_{33} = 1.386$, $P = .18$) Cr concentrations. Again, the ratio of gray matter to white matter Cr concentration was similar for the 3 groups (young control group ratio = 1.98; elderly control group ratio = 1.95; and AD group ratio = 2.12) ($F_{2,49} = 1.503$, $P = .23$).

Table 1. Characteristics of Patients With Alzheimer Disease

Subject*/ Age, y/Sex	MMSE† Score	Medications
1/69/F	15	Nizatidine, donepezil, hydrochlorothiazide, estrogen, Vancenase (beclomethasone dipropionate) nasal spray, aspirin, vitamin supplements
2/65/F	20	L-Carnitine, estrogen, and over-the-counter health food and vitamin supplements
3/76/F	21	Estrogen and aspirin
4/73/M	24	Lorazepam and over-the-counter vitamin supplements
5/79/F	15	Sertraline hydorchloride, hydrochlorothiazide, lisinorpril, levothyroxine sodium, timolol optic, promethazine hydrochloride, and over-the-counter antihistamines
6/72/F	18	L-Carnitine, estrogen and acetaminophen
7/79/M	21	None
8/84/F	17	Furosemide, estrogen, meclizine hydrochloride, and metoprolol
9/73/M	20	Donepezil and vitamin E
10/73/F	24	Estrogen, donepezil, over-the-counter health food and vitamin supplements
11/77/F	26	Progesterone, estrogen, folic acid, melatonin, tacrine hydrochloride, hydrochlorothiazide, L-Carnitine, and over-the-counter health food
12/77/M	16	None
13/68/M	24	Glyburide, atorvastatin calcium and donepezil
14/78/F	11	L-Carnitine, hydrochlorothiazide, theophylline, and naphazoline hydrochloride
15/71/F	17	None
16/60/M	28	L-Carnitine

**Patient 3 had Crohn disease; patient 5 had depression; patient 8 had past depression and anxiety; and patient 16 had past alcoholism, with 18 years of sobriety.*

†MMSE indicates Mini-Mental State Examination.

For Cho concentrations, a repeated-measures analysis of variance (3 groups by 2 tissue types) yielded a significant group effect ($F_{2,47} = 10.964$, $P = .001$) and interaction ($F_{2,47} = 12.073$, $P = .001$) and trend toward a tissue-type effect ($F_{1,47} = 3.691$, $P = .06$). Gray matter Cho concentrations were lowest in the young controls and highest in the patients with AD, and all group-paired comparisons were significant (young vs elderly: $t_{32} = 3.925$, $P = .001$; elderly vs patients with AD: $t_{33} = 2.506$, $P = .02$; young vs patients with AD: $t_{29} = 4.993$, $P = .001$). As indicated by the interaction, white matter Cho showed a different pattern from gray matter; only the comparison between the elderly controls and patients with AD reached significance; the elderly group had higher Cho concentrations than the AD group ($t_{33} = 3.074$, $P = .004$). Unlike NAc and Cr, the ratio of gray matter to white matter for Cho concentration showed a group difference, with the value for the AD group higher (ratio = 1.20) than values for the young (ratio = .79, $t_{29} = 4.061$, $P = .001$) and elderly control (ratio = .91, $t_{33} = 3.362$, $P = .002$) groups; the young and elderly controls did not differ significantly from each other ($t_{32} = 1.351$, $P = .19$).

The 3 group-by-metabolite analyses of variance were recalculated excluding women, because the younger group was composed of men only. The results were the same without the women, except that the group-by-Cr interaction was no longer significant in the men-only analysis.

CORRELATIONS BETWEEN METABOLITE CONCENTRATIONS AND COGNITIVE TEST SCORES

As expected, the AD group was impaired on the 3 cognitive measures compared with the elderly controls (**Table 3**). There were several brain-behavior cor-

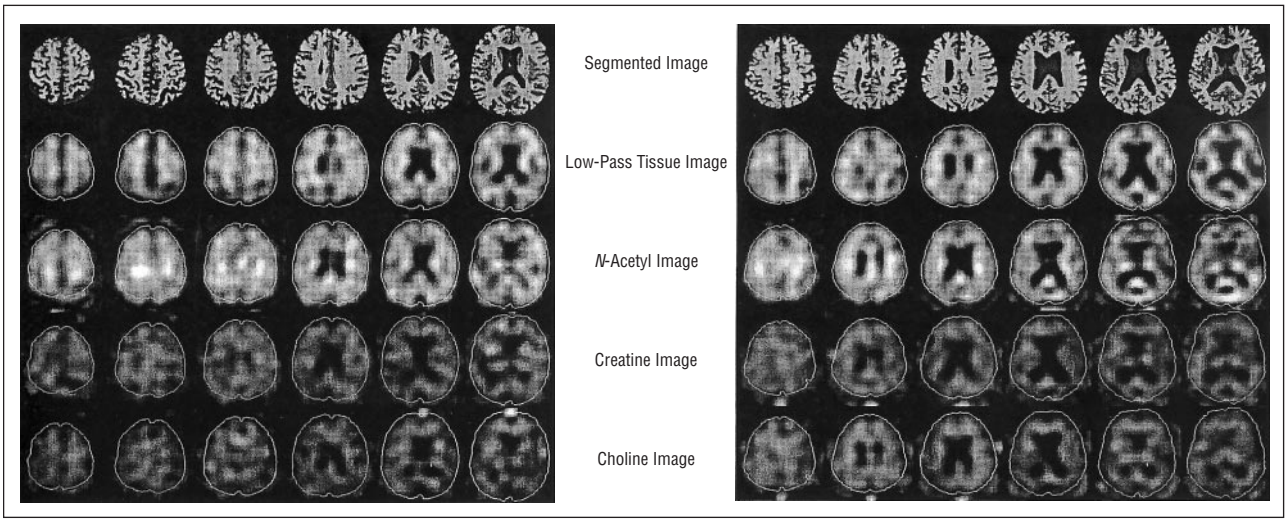

Figure 1. *Left, Brain images of a 73-year-old male control. Right, Brain images of a 75-year-old male patient with Alzheimer disease. Superior to inferior brain slices are shown from left to right. Segmented image: the fast spin-echo magnetic resonance structural images are segmented into cerebrospinal fluid (dark gray), gray matter (medium gray), and white matter (light gray). Low-pass tissue image: The tissue image after low-pass filtering matches the spatial frequency characteristics of the metabolite images. The white outlines on these and the specific metabolite images below are taken from the perimeter of the structural images and indicate the registration of the metabolite image with the structural image. Images of* N*-acetyl compounds, creatine, and choline are of signal intensities that contribute to the quantification of each metabolite concentration.*

relations in the predicted direction. In elderly controls, face recognition scores were positively correlated with gray matter NAc concentration ($r = 0.80$, $P = .001$, n = 13). In patients with AD, higher Cr gray matter concentrations were related to lower word-recognition scores ($r = -0.67$, $P = .03$, n = 11), and higher Cho gray matter concentrations were related to lower face recognition scores ($r = -0.70$, $P = .02$, n = 11).

COMMENT

Independent estimation of the concentrations of NAc, Cr, and Cho revealed different patterns across the groups: NAc showed a disease effect, Cr showed an age effect, and Cho showed disease and age effects. *N*-Acetyl compounds concentration was significantly reduced only in AD in gray matter but not white matter, even though both the AD and elderly control groups had substantial gray matter volume deficits relative to the young controls. Both the elderly healthy and AD groups had an excess of Cr in gray matter. Choline concentration in gray matter was notably higher in the elderly than in the young control group, and the AD values were even higher than those measured in the elderly controls.

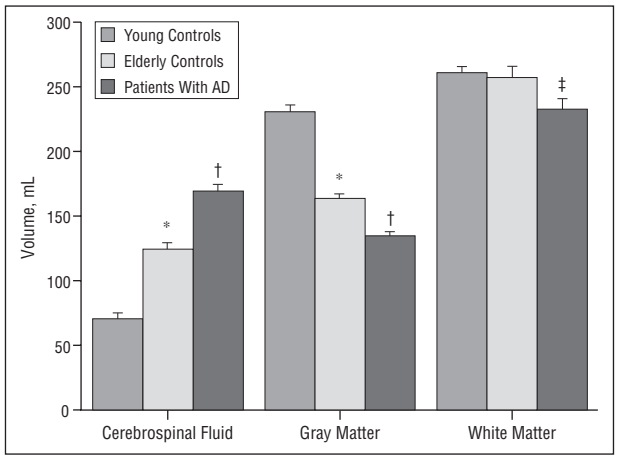

Figure 2. *Volumes, without metabolite criteria imposed, derived from the segmented magnetic resonance imaging structural data for each of the compartments. The 3 groups showed a stepwise increase in brain cerebrospinal fluid volume, where the young controls had the smallest volume and the patients with Alzheimer disease (AD) the largest volume; all pairwise differences were significant. Gray matter volume showed the complementary pattern of group differences. White matter volume, however, was deficient only in the AD group relative to the young and elderly control groups. Error bars indicate SEMs (young vs elderly* P≤.001; elderly vs AD †P≤.001, ‡P = .06). Please refer to Table 2 for* t *test results.*

While neuronal soma and processes may shrink, the current consensus is that little if any loss of neuronal cell numbers occurs in normal aging.[26-29] Gray matter volume deficits without NAc concentration deficit suggests normal cell integrity in the healthy elderly. Like postmortem studies,[10,16-20,28] the current in vivo study revealed severe gray matter volume deficits and an accompanying deficit in gray matter NAc concentration in AD.

For literature comparison, we calculated whole brain raw signal intensity NAc/Cr ratio values of 1.382, 1.274, and 1.225 for the young, elderly, and AD groups, respectively. Concentration-corrected ratios of NAc/Cr for gray matter only presented a similar pattern of 1.38, 1.229, and 1.098 for the young, elderly, and AD groups, whereas for white matter only the pattern was 2.073, 1.734, 1.743. Thus, the NAc/Cr ratio differences seen in whole-brain mixed gray-white tissue represent a decrease in the NAc/Cr ratio with aging but no additional AD effect in white matter and a further decrease in this ratio in the AD group in gray matter.

Consistent with other in vivo[31,44-47,70-72] and ex vivo or postmortem[33,54,73,74] reports, NAc concentration, whether expressed as a ratio of Cr or Cho or in absolute terms, was substantially lower in patients with AD than in age-matched controls. Kwo-On-Yeun et al[54] also noted substantially more reduction in NAc in gray matter than in white matter in comparing patients with AD to controls. As in other studies, NAc signal intensity was greater in gray matter than white matter for all 3 groups in our study.

Across all 3 groups, the calculated Cr concentration in gray matter was almost twice that in white matter, whereas the Cho concentration was more uniformly distributed between gray and white matter. Given these age- and disease-related differences in metabolite con-

Table 2. Structural Composition (mL) of Brain Generating Magnetic Resonance Spectroscopy Signal (Mean ± SE)

Characteristics	Young Controls	Young Controls vs Elderly Controls	Elderly Controls	Elderly Controls vs Patients With AD*	Patients With AD
With Metabolite Criteria					
Cerebrospinal fluid	40.6 ± 2.91	$t_{32} = 6.421$, $P<.001$	71.3 ± 3.57	$t_{33} = 4.562$, $P<.001$	99.9 ± 5.35
Gray matter	151.9 ± 6.05	$t_{32} = 6.043$, $P<.001$	106.9 ± 4.58	$t_{33} = 3.756$, $P = .001$	84.8 ± 3.39
White matter	208.0 ± 7.96	$t_{32} = .734$, $P = .47$	198.4 ± 9.78	$t_{33} = 1.938$, $P < .07$	173.8 ± 7.48
Without Metabolite Criteria					
Cerebrospinal fluid	69.8 ± 4.11	$t_{32} = 8.206$, $P<.001$	124.3 ± 4.92	$t_{33} = 5.119$, $P <.001$	168.7 ± 7.44
Gray matter	231.6 ± 4.06	$t_{32} = 11.52$, $P<.001$	163.3 ± 4.18	$t_{33} = 4.558$, $P <.001$	133.2 ± 5.21
White matter	261.2 ± 5.09	$t_{32} = .294$, $P = .77$	257.9 ± 8.94	$t_{33} = 1.966$, $P < .06$	234.2 ± 7.76

**AD indicates Alzheimer disease.*

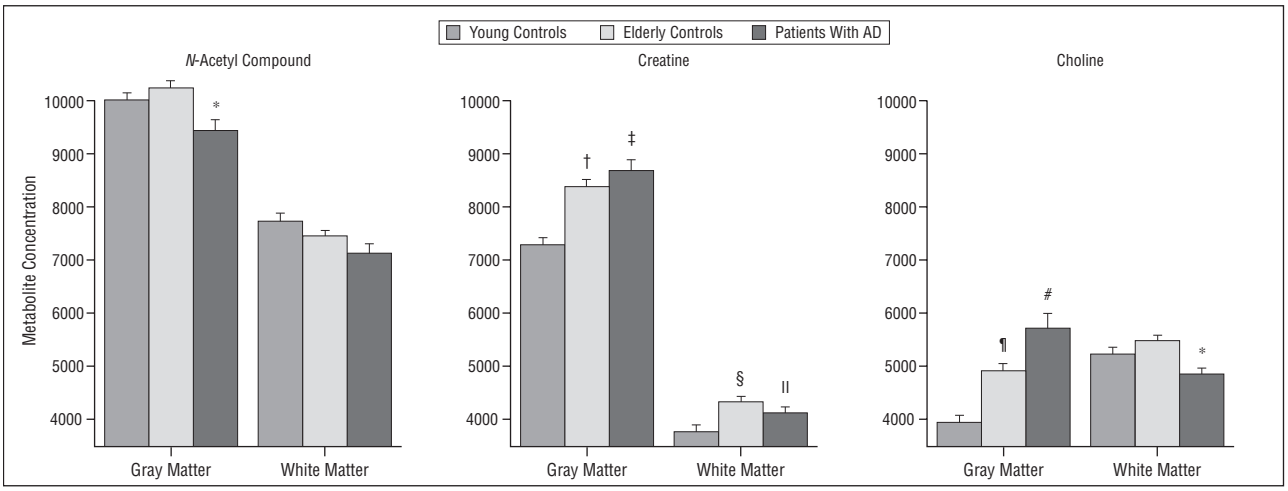

Figure 3. *Concentrations in gray matter and white matter for each brain metabolite measured. Relative to the elderly control group, the Alzheimer disease (AD) group had lower* N*-acetyl compounds concentrations in gray matter (*$t_{33} = 2.771$, P = .01) but not white atter ($t_{33} = 1.419$, P = .17). Creatine was higher in the gray matter of elderly controls (†$t_{32} = 4.647$, P = .0001) and patients with AD (‡$t_{29} = 4.804$, P = .001) and in the white matter of elderly controls (§$t_{32} = 3.603$, P = .002) and patients with AD(‖$t_{29} = 2.133$, P = .04) relative to the young controls, showing an age effect. Choline showed an additive age and disease effect for gray matter (¶ young vs elderly: $t_{32} = 3.847$, P = .02; #elderly vs AD: $t_{33} = 2.552$, P = .005). Error bars indicate SEMs.*

Table 3. Scores on Cognitive Tests

Tests	Elderly Controls Mean (SE)	Elderly Controls No. of Subjects	Elderly Controls Patients With AD*	Patients With AD,† Mean (SE)
Modified Boston Naming Test	38.3 (1.2)	8	$t_{17} = 2.797$, $P<.02$	28.3 (2.9)
Warrington Recognition Test				
Words	46.8 (1.1)	13	$t_{22} = 8.421$, $P<.001$	30.2 (1.7)
Faces	42.3 (1.2)	13	$t_{22} = 4.673$, $P<.001$	31.3 (2.2)

**AD indicates Alzheimer disease.*
†n = 11.

centrations for gray and white matter, it is clear that neither Cr nor Cho concentration is constant, and, thus, they should not be used without regard to age and disease effects as referents in ratio expression of the NAc signal. The 3 group comparisons—young controls, elderly controls, and elderly patients with AD—help to disentangle disease effects from effects of normal aging. The former should be superimposed on the latter. Patients with AD did not significantly differ from the elderly controls in the volume of Cr in either gray or white matter, but both groups differed from the young controls. This pattern indicates that increased Cr concentration in patients with AD is attributable to advanced age rather than to the disease. The elevated gray matter Cho concentration in AD, however, seems to be the result of the additive effects of advanced age plus disease. Chang et al[39] noted decreased brain water content (noncerebrospinal fluid) with age, which could explain a relative decrease in cortical volume with the same number of cells, leading to increased metabolite concentration. Miller et al[49] reported that increased choline reflects degree of cellular density in brain tumors. Adding gliosis to this aging effect could explain the additional increase in Cho level we observed in patients with AD. White matter Cho concentration showed the opposite pattern, ie, no increase with age but a decrease with AD. Moats et al[71] observed age-related increases in Cho levels in normal elderly but no further differences between normal elderly and patients with AD. Our observed increased Cho concentration in gray matter may be the result of cell membrane turnover.

Pettegrew et al,[75] using in vitro phosphorus 31 (^{31}P) MRS, found elevated phosphomonoester levels in patients with AD. Brown et al[76] showed that phosphomonoester, phosphomonoester/phosphodiesther, and inorganic phosphate levels were elevated in patients with AD compared with controls, whereas no significant differences in any ^{31}P indexes were found by Bottomley et al.[77] Similar findings were reported by Murphy et al.[78] More recently, Gonzalez et al[79] reported a 50% increase in phosphomonoester/phosphoiesther levels in patients with AD, but unchanged β-nucleoside 5′-triphosphate, phosphocreatine, and inorganic phosphate levels in AD, speculating that the phosphodiesther difference reflected changes in the biophysical state of membrane phospholipids. Using quantitative ^{31}P and ^{1}H perchloric acid extracts, Klunk et al[80] found increased myoinositol, aspartate, L-glutamate, alanine, phosphocholine, and phosphodiester levels, and decreased phosphoetanolamine and NAc-L-aspartate levels. They concluded that compounds related to membrane degradation and excitatory neurotransmission increased in patients with AD, while those related to neuronal integrity and inhibitory neurotransmission decreased. Pettegrew et al[81] reported

increased phosphomonoesther and phosphocreatine levels that preceded dementia for 1 subject.

The proton Cr signal is a combination of phosphocreatine and creatine.[82] Thus, one cannot separate the contribution of creatine and phosphocreatine to the total Cr signal or relate findings directly to phosphorus spectroscopy studies, which, for instance, report a decreased ratio of phosphocreatine to inorganic orthophosphate in AD.[83] Similarly, several Cho-containing compounds contribute to the Cho peak in proton magnetic resonance spectroscopy. As reviewed by Michaelis et al[82] Cho plasmogen (0.6 mmol/kg), glycerophosphorylcholine (0.4 mmol/kg), phosphorylcholine (0.4 mmol/kg), cytedinediphosphate-choline (0.05 mmol/kg), acetylcholine (0.03 mmol/kg), and choline (0.02 mmol/kg) contribute to the ^{1}MRS choline signal. Contributions from 15- to 18-mmol/L lipid-soluble phosphatidylcholine are minor.[49,82] In vivo ^{31}P MRS could clearly play an important role in identifying the sources of the observed Cho as well as Cr signals in ^{1}H MRSI.

A limitation of our method is imposed by the inhomogeneity of the main magnetic field. While we applied second-order, nonlinear shims to improve the homogeneity, the remaining field inhomogeneities, particularly in the more inferior and frontal brain regions, limit the useful extent of the observed volume. Because we apply a late-echo acquisition, metabolites with short T_2 relaxation times, such as myoinositol, are not observed.

The level of brain metabolite concentration seen with ^{1}H MRSI appears to have functional significance, given the correlations found with cognitive measures. The metabolite concentration–memory test correlations are consistent with our previous work, which showed a selective relationship between these tests and degree of hippocampal volume loss in patients with AD.[3,6] Together, these results lend support to the hypothesis that the prominent disease-related increase in gray matter Cho concentration marks cellular degeneration resulting in reduced NAc concentration and poorer cognitive function in AD.

Accepted for publication October 2, 1998.

This work was supported by grants AG11427, AA05965, and MH30854 (Dr Pfefferbaum), AA10723 and MH40041 (Dr Sullivan), and RR09784 and CA48269 (Dr Spielman) from the National Institutes of Health, Bethesda, Md.

We thank the the State of California Alzheimer's Disease Research Center, Veterans Affairs Palo Alto Health Care System, Palo Alto, Calif, for providing subjects for the study.

Corresponding author: Adolf Pfefferbaum, MD, Neuropsychiatry Program (BN166), SRI International, 333 Ravenswood Ave, Menlo Park, CA 94025 (e-mail: dolf@synapse.sri.com).

REFERENCES

1. Tanabe JL, Amend D, Schuff N, DiSclafani V, Ezekiel F, Norman D, Fein G, Weiner MW. Tissue segmentation of the brain in Alzheimer disease. *AJNR Am J Neuroradiol*. 1997;18:115-123.
2. Rusinek H, De Leon MJ, George AE, Stylopoulos LA, Chandra R, Smith G, Rand T, Mourino M, Kowalski H. Alzheimer disease: measuring loss of cerebral gray matter with MR imaging. *Radiology*. 1991;178:109-114.
3. Fama R, Sullivan EV, Shear PK, Marsh L, Yesavage JA, Tinklenberg JR, Lim KO, Pfefferbaum A. Selective cortical and hippocampal volume correlates of Mattis Dementia Rating Scale in Alzheimer disease. *Arch Neurol*. 1997;54:719-728.
4. Jernigan TL, Salmon DP, Butters N, Shults CW, Hesselink JR. Specificity of brain-structural changes in Alzheimer's, Huntington's, and Parkinson's diseases. *J Clin Exp Neuropsychol*. 1990;12:410.
5. De Leon MJ, George AE, Stylopoulos LA, Smith G, Miller DC. Early marker for Alzheimer's disease: the atrophic hippocampus. *Lancet*. 1989;2:672-673.
6. Cahn DA, Sullivan EV, Shear PK, Marsh L, Fama R, Lim KO, Yesavage JA, Tinklenberg JR, Pfefferbaum A. Structural MRI correlates of recognition memory in Alzheimer's disease. *J Int Neuropsychol Soc*. 1998;4:106-114.
7. Soininen HS, Partanen K, Pitkanen A, Vainio P, Hanninen T, Hallikainen M, Koivisto K, Riekkinen PJ. Volumetric MRI analysis of the amygdala and the hippocampus in subjects with age-associated memory impairment: correlation to visual and verbal memory. *Neurology*. 1994;44:1660-1668.
8. Seab JP, Jagust WJ, Wong STS, Roos MS, Reed BR, Budinger TF. Quantitative NMR measurements of hippocampal atrophy in Alzheimer's disease. *Magn Reson Med*. 1988;8:200-208.
9. Bouras C, Hof PR, Morrison JH. Neurofibrillary tangle densities in the hippocampal formation in a non-demented population define subgroups of patients with differential early pathologic changes. *Neurosci Lett*. 1993;153:131-135.
10. Kemper TL. Neuroanatomical and neuropathological changes during aging and dementia. In: Albert, ML, Knoefel, JE, eds. *Clinical Neurology of Aging*. New York, NY: Oxford University Press; 1994.
11. Brun A, Englund E. The pattern of degeneration in Alzheimer's disease: neuronal loss and histopathological grading. *Histopathology*. 1981;5:549-564.
12. Brun A, Gustafson L, Englund E. Subcortical pathology of Alzheimer's disease. *Alzheimer Dis Assoc Disord*. 1990;51:73-77.
13. Braak H, Braak E. Alzheimer's disease affects limbic nuclei of the thalamus. *Acta Neuropathol (Berl)*. 1991;81:261-268.
14. Braak H, Braak E. Neuropathological staging of Alzheimer-related changes. *Acta Neuropathol (Berl)*. 1991;82:239-259.
15. Hof PR. Morphology and neurochemical characteristics of the vulnerable neurons in brain aging and Alzheimer's disease. *Eur Neurol*. 1997;37:71-81.
16. Arnold SE, Hyman BT, Van Hoesen G. Neuropathological changes of the temporal pole in Alzheimer's disease and Pick's disease. *Arch Neurol*. 1994;51:145-150.
17. Mufson EJ. Lack of neocortical nerve cell loss in Alzheimer's disease: reality or methodological artifact. *Neurobiol Aging*. 1994;15:361-362.
18. Braak H, Braak E. Morphological criteria for the recognition of Alzheimer's disease and the distribution pattern of cortical changes related to this disorder. *Neurobiol Aging*. 1994;15:355-356.
19. Regeur L, Jensen GB, Pakkenberg H, Evans SM, Pakkenberg B. No global neocortical nerve cell loss in brains from patients with senile dementia of Alzheimer's type. *Neurobiol Aging*. 1994;15:347-352.
20. Swaab DF, Hofman MA, Lucassen PJ, Salehi A, Uylings HBM. Neuronal atrophy, not cell death, is the main hallmark of Alzheimer's disease. *Neurobiol Aging*. 1994; 15:369-371.
21. Pfefferbaum A, Mathalon DH, Sullivan EV, Rawles JM, Zipursky RB, Lim KO. A quantitative magnetic resonance imaging study of changes in brain morphology from infancy to late adulthood. *Arch Neurol*. 1994;51:874-887.
22. Raz N, Gunning FM, Head D, Dupuis JH, McQuain J, Briggs SD, Loken WJ, Thornton AE, Acker JD. Selective aging of the human cerebral cortex observed in vivo: differential vulnerability of the prefrontal gray matter. *Cereb Cortex*. 1997;7:268-282.
23. Blatter DD, Bigler ED, Gale SD, Johnson SC, Anderson C, Burnett BM, Parker N, Kurth S, Horn S. Quantitative volumetric analysis of brain MRI: normative database spanning 5 decades of life. *Am J Neuroradiol*. 1995;16:241-245.
24. Jernigan TL, Archibald SL, Berhow MT, Sowell ER, Foster DS, Hesselink JR. Cerebral structure on MRI, I: localization of age-related changes. *Biol Psychiatry*. 1991;29:55-67.
25. Guttmann CRG, Jolesz FA, Kikinis R, Killiany RJ, Moss MB, Sandor T, Albert MS. White matter changes with normal aging. *Neurology*. 1998;50:972-978.
26. Tang Y, Nyengaard JR, Pakkenberg B, Gundersen HJG. Age-induced white-matter changes in the human brain: a stereological investigation. *Neurobiol Aging*. 1997;18:609-615.
27. Flood DG, Coleman PD. Hippocampal plasticity in normal aging and decreased plasticity in Alzheimer's disease. In: Storm-Mathisen J, Zimmer J, Otterson OP, eds. *Progress in Brain Research: Understanding the Brain Through the Hippocampus*. Amsterdam, the Netherlands: Elsevier Science Publishers; 1990;83: 435-443.
28. Flood DG. Region-specific stability of dendritic extent in normal human aging and regression in Alzheimer's disease, II: subiculum. *Brain Res*. 1991;540:83-95.
29. Flood DG. Critical issues in the analysis of dendritic extent in aging humans, primates, and rodents. *Neurobiol Aging*. 1993;14:649-654.
30. Tallan HH. Studies on the distribution of *N*-acetyl-L-aspartate acid in brain. *J Biol Chem*. 1956;224:41-45.
31. Ernst T, Chang L, Melchor R, Mehringer CM. Frontotemporal dementia and early Alzheimer disease: differentiation with frontal lobe H-1 NTR spectroscopy. *Radiology*. 1997;203:829-836.
32. Schuff N, Amend D, Ezekiel F, Steinman SK, Tanabe J, Norman D, Jagust W, Kramer JH, Mastrianni JA, Fein G, Weiner MW. Changes of hippocampal *N*-acetyl aspartate and volume in Alzheimer's disease: a proton MR spectroscopic imaging and MRI study. *Neurology*. 1997;49:1513-1521.
33. Klunk WE, Panchalingam K, Moossy J, McClure RJ, Pettegrew JW. *N*-acetyl-L-aspartate and other amino acid metabolites in Alzheimer's disease brain: a preliminary proton nuclear magnetic resonance study. *Neurology*. 1992;42:1578-1585.

34. Lim KO, Spielman DM. Estimating NAA in cortical gray matter with applications for measuring changes due to aging. *Magn Reson Med*. 1997;37:372-377.
35. Charles HC, Lazeyras F, Krishnan KRR, Boyko OB, Patterson LJ, Doraiswamy PM, McDonald WM. Proton spectroscopy of human brain: effects of age and sex. *Prog Neuropsychopharmacol Biol Psychiatry*. 1994;18:995-1004.
36. Fukuzako H, Hashiguchi T, Sakamoto Y, Okamura H, Doi W, Takenouchi K, Takigawa M. Metabolite changes with age measured by proton magnetic resonance spectroscopy in normal subjects. *Psychiatry Clin Neurosci*. 1997;51:261-263.
37. Christiansen P, Toft P, Larsson HBW, Stubgaard M, Henriksen O. The concentration of *N*-acetyl aspartate, creatine+phosphocreatine, and choline in different parts of the brain in adulthood and senium. *Magn Reson Imaging*. 1993;11:799-806.
38. Pfefferbaum A, Sullivan E, Adalsteinsson A, Spielman D, Lim KO. In vivo quantification of *N*-acetyl aspartate, creatine and choline from large volumes of gray and white matter on magnetic resonance spectroscopic imaging: application to normal aging. *Magn Reson Med*. 1999;41:276-294.
39. Chang L, Ernst T, Poland RE, Jenden DJ. In vivo proton magnetic resonance spectroscopy of the normal aging human brain. *Life Sci*. 1996;58:2049-2056.
40. Meyerhoff DJ, MacKay S, Constans JM, Norman D, Van Dyke C, Fein G, Weiner MW. Axonal injury and membrane alterations in Alzheimer's disease suggested by in vivo proton magnetic resonance spectroscopic imaging. *Ann Neurol*. 1994;36:40-47.
41. Soher BJ, van Zijl PCM, Duyn JH, Barker PB. Quantitative proton MR spectroscopic imaging of the human brain. *Magn Reson Med*. 1996;35:356-363.
42. Kreis R, Ernst T, Ross BD. Absolute quantitation of water and metabolites in the human brain, II: metabolite concentrations. *J Magn Reson*. 1993;102:9-19.
43. Saunders DE, Howe FA, van den Boogaart A, Griffith JR, Brown MM. Aging of the human adult brain: in vivo quantification of metabolic content with proton magnetic resonance spectroscopy [abstract]. *Proc Soc Magn Reson*. 1995;3:1804.
44. Parnetti L, Tarducci R, Presciutti O, Lowenthal DT, Pippi M, Palumbo B, Gobbi G, Pelliccioli GP, Senin U. Proton magnetic resonance spectroscopy can differentiate Alzheimer's disease from normal aging. *Mech Ageing Dev*. 1997;97:9-14.
45. Frederick BD, Satlin A, Yurgelun-Todd DA, Renshaw PF. In vivo proton magnetic resonance spectroscopy of Alzheimer's disease in the parietal and temporal lobes. *Biol Psychiatry*. 1997;42:147-150.
46. Kattapong VJ, Brooks WM, Wesley MH, Kodituwakku PW, Rosenberg GA. Proton magnetic resonance spectroscopy of vascular- and Alzheimer-type dementia. *Arch Neurol*. 1996;53:678-680.
47. Tedeschi G, Bertolino A, Lundbom N, Bonavita S, Patronas NJ, Duyn JH, Metman LV, Chase TN, Di Chiro G. Cortical and subcortical chemical pathology in Alzheimer's disease as assessed by multislice proton magnetic resonance spectroscopic imaging. *Neurology*. 1996;47:696-704.
48. Tedeschi G, Lundbom N, Raman R, Bonavita S, Duyn J, Alger J, Di Chiro G. Increased choline signal coinciding with malignant degeneration of cerebral gliomas: a serial proton magnetic resonance spectroscopy imaging study. *J Neurosurg*. 1997;87:516-524.
49. Miller BL, Chang L, Booth R, Ernst T, Cornford M, Nikas D, McBride D, Jenden DJ. In vivo H-1 MRS choline: correlation with in vitro chemistry histology. *Life Sci*. 1996;58:1929-1935.
50. Moyher SE, Nelson SJ, Wald LL, Henry RG, Kurhanewicz J, Vigneron DB. High-spatial resolution MRS and segmented MRI to study NAA in cortical gray matter and white matter of the human brain [abstract]. *Proc Soc Magn Reson*. 1995;1:332.
51. Narayana PA, Fotedar LK, Jackson EF, Bohan TP, Butler IJ, Wolinsky JS. Regional in vivo proton magnetic resonance spectroscopy of brain. *J Magn Reson*. 1989;83:44-52.
52. Wang Y, Li S-J. Differentiation of metabolic concentrations between gray matter and white matter of human brain by in vivo 1H magnetic resonance spectroscopy. *Magn Reson Med*. 1998;39:28-33.
53. Doyle TJ, Beddell BJ, Narayana PA. Relative concentration of proton MR visible neurochemicals in gray and white matter in human brain. *Magn Reson Med*. 1995;33:755-759.
54. Kwo-On-Yuen PF, Newmark RD, Budinger TF, Kaye JA, Ball MJ, Jagust WJ. Brain *N*-acetyl-L-aspartic acid in Alzheimer's disease: a proton magnetic resonance spectroscopy study. *Brain Res*. 1994;667:167-174.
55. Petroff OA, Spencer DD, Alger JR, Prichard JW. High-field proton magnetic resonance spectroscopy of human cerebrum obtained during surgery for epilepsy. *Neurology*. 1989;39:1197-1202.
56. Petroff OAC, Pleban LA, Spencer DD. Symbiosis between in vivo and in vitro NMR spectroscopy: the creatine, *N*-acetylaspartate, glutamate and GABA content of the epileptic human brain. *Magn Reson Imaging*. 1995;13:1197-1211.
57. Tedeschi G, Bertolino A, Righini A, Campbell G, Raman R, Duyn JH, Moonen CTW, Alger JR, Di Chiro G. Brain regional distribution pattern of metabolite signal intensities in young adults by proton magnetic resonance spectroscopic imaging. *Neurology*. 1995;45:1384-1391.
58. Pouwels PJW, Frahm J. Regional metabolite concentrations in human brain as determined by quantitative localized proton MRS. *Magn Reson Med*. 1998;39:53-60.
59. Hetherington HP, Pan JW, Mason GF, Adams D, Vaughn MJ, Tweig DB, Pohost GM. Quantitative ^{1}H spectroscopic imaging of human brain at 4.1 T using image segmentation. *Magn Reson Med*. 1996;36:21-29.
60. Knufman NMJ, Berkelbach, van der Sprenkel JW, Tulleken CAF. *N*-Acetylaspartate differences between gray and white matter as observed by proton spectroscopic imaging in normal subjects [abstract]. *Proc Soc Magn Reson*. 1992;1905.
61. McKhann G, Drachman D, Folstein M, Katzman R. Clinical diagnosis of Alzheimer's disease: report of the NINCDS-ADRDA Work Group under the auspices of Department of Health and Human Services Task Force on Alzheimer's disease. *Neurology*. 1984;37:939-944.
62. Khachaturian ZS. Diagnosis of Alzheimer's disease. *Arch Neurol*. 1985;42:1097-1105.
63. Folstein MF, Folstein SE, McHugh PR. Mini-Mental State: a practical method for grading the cognitive state of patients for the clinician. *J Psychiatr Res*. 1975;12:189-198.
64. Warrington E. *Recognition Memory Test Manual*. Windsor, England: Nelson Publishing Co; 1984.
65. Huff FJ, Collins C, Corkin S, Rosen TJ. Equivalent forms of the Boston Naming Test. *J Clin Exp Neuropsychol*. 1986;8:556-562.
66. Adalsteinsson E, Irarrazabal P, Spielman DM, Macovski A. Three-dimensional spectroscopic imaging with time-varying gradients. *Magn Reson Med*. 1995;33:461-466.
67. Spielman D, Adalsteinsson E, Lim KO. Quantitative analysis of improved homogeneity using linear versus higher order shims for CSF of the brain [abstract]. In: Abstracts of the Fifth Scientific Meeting of the International Society for Magnetic Resonance in Medicine; April 12-18, 1997; Vancouver, British Columbia.
68. Webb P, Macovski A. Rapid, fully-automatic, arbitrary volume, in-vivo shimming. *Magn Reson Med*. 1991;20:113-122.
69. Gudbjartsson H, Patz S. The Rician distibution of noisy MRI data. *Magn Reson Med*. 1995;34:910-914.
70. MacKay S, Meyerhoff DJ, Constans JM, Norman D, Fein G, Weiner MW. Regional gray and white matter metabolite differences in subjects with AD, with subcortical ischemic vascular dementia, and elderly controls with H-1 magnetic resonance spectroscopic imaging. *Arch Neurol*. 1996;53:167-174.
71. Moats RA, Ernst T, Shonk TK, Ross BD. Abnormal cerebral metabolite concentrations in patients with probable Alzheimer's disease. *Magn Reson Med*. 1994;32:110-115.
72. Mohanakrishnan P, Fowler AH, Vonsattel JP, Jolles PR, Husain MM, Liem P, Myers L, Komoroski RA. Regional metabolic alterations in Alzheimer's disease: an in vitro H-1 NMR study of the hippocampus and cerebellum. *J Gerontol A Biol Sci Med Sci*. 1997;52:B111-B117.
73. Jaarsma D, Veenma van der Duin L, Korf J. *N*-acetylaspartate and *N*-acetylaspartylglutamate levels in Alzheimer's disease post-mortem brain tissue. *J Neurol Sci*. 1994;127:230-233.
74. Mohanakrishnan P, Fowler AH, Vonsattel JP, Husain MM, Jolles PR, Liem P, Komoroski RA. An in vitro H-1 nuclear magnetic resonance study of the temporoparietal cortex of Alzheimer brains. *Exp Brain Res*. 1995;102:503-510.
75. Pettegrew J, Moossy J, Withers G, McKeag D, Panchalingam K. 31P nuclear magnetic resonance study of the brain in Alzheimer's disease. *J Neuropathol Exp Neurol*. 1988;47:235-248.
76. Brown G, Levine S, Gorell J, Pettegrew J, Gdowski J, Bueri J, Helpern J, Welch K. In vivo 31P NMR profiles of Alzheimer's disease and multiple subcortical infarct dementia. *Neurology*. 1989;39:1423-1427.
77. Bottomley PA, Cousins JP, Pendrey DL, Wagle WA, Hardy CJ, Eames FA, McCaffrey RJ, Thompson DA. Alzheimer dementia: quantification of energy metabolism and mobile phosphoesters with P-31 NMR spectroscopy. *Radiology*. 1992;183:695-699.
78. Murphy DGM, Bottomley PA, Salerno JA, DeCarli C, Mentis MJ, Grady CL, Teichberg D, Giacometti KR, Rosenberg JM, Hardy CJ, Schapiro MB, Rapoport SI, Alger JR, Horwitz B. An in vivo study of phosphorus and glucose metabolism in Alzheimer's disease using magnetic resonance spectroscopy and PET. *Arch Gen Psychiatry*. 1993;50:341-349.
79. Gonzalez RG, Guimaraes AR, Moore GJ, Crawley A, Cupples LA, Growdon JH. Quantitative in vivo P-31 magnetic resonance spectroscopy of Alzheimer disease. *Alzheimer Dis Assoc Dis*. 1996;10:46-52.
80. Klunk WE, Xu C, Panchalingam K, McClure RJ, Pettegrew JW. Quantitative H-1 and P-31 MRS of PCA extracts of postmortem Alzheimer's disease brain. *Neurobiol Aging*. 1996;17:349-357.
81. Pettegrew JW, Klunk WE, Kanal E, Panchalingam K, McClure RJ. Changes in brain membrane phospholipid and high-energy phosphate metabolism precede dementia. *Neurobiol Aging*. 1995;16:973-975.
82. Michaelis T, Merboldt KD, Bruhn H, Hanicke W, Frahm J. Absolute concentrations of metabolites in the adult human brain in vivo: quantification of localized proton MR spectra. *Radiology*. 1993;187:219-227.
83. Smith CD, Pettigrew LC, Avison MJ, Kirsch JE, Tinkhtman AJ, Schmitt FA, Wermeling DP, Wekstein DR, Markesberry WR. Frontal lobe phosphorus metabolism and neuropsychological function in aging and in Alzheimer's disease. *Ann Neurol*. 1995;38:194-201.